ResearchGate

See discussions, stats, and author profiles for this publication at: http://www.researchgate.net/publication/280738964

Experimental and Numerical Investigation on the Effect of Cooling/Heating Rate on the Freeze-Thaw Behavior of Mortar Containing Deicing Salt Solution

CONFERENCE PAPER · JUNE 2015

DOWNLOADS
20

VIEWS
76

5 AUTHORS, INCLUDING:


Hadi Shagerdi
Purdue University
1 PUBLICATION **0** CITATIONS
SEE PROFILE

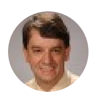
D. P. Bentz
National Institute of Standards and Technolo…
317 PUBLICATIONS **5,365** CITATIONS
SEE PROFILE


Pablo D Zavattieri
Purdue University
59 PUBLICATIONS **1,570** CITATIONS
SEE PROFILE


William Jason Weiss
Purdue University
221 PUBLICATIONS **1,810** CITATIONS
SEE PROFILE

Available from: Yaghoob Farnam
Retrieved on: 19 August 2015

Experimental and Numerical Investigation on the Effect of Cooling/Heating Rate on the Freeze-Thaw Behavior of Mortar Containing Deicing Salt Solution

Yaghoob Farnam[1], Hadi Shagerdi Esmaeeli[2], Dale Bentz[3], Pablo Zavattieri[4], and Jason Weiss[5]

[1]Graduate Research Assistant, Lyles School of Civil Engineering, Purdue University, 550 Stadium Mall Dr., West Lafayette, IN 47907, USA, yfarnam@purdue.edu.

[2]Graduate Research Assistant, Lyles School of Civil Engineering, Purdue University, 550 Stadium Mall Dr., West Lafayette, IN 47907, USA, hshagerd@purdue.edu.

[3]Chemical Engineer, Materials and Structural Systems Division, National Institute of Standards and Technology, 100 Bureau Drive, Stop 8615, Gaithersburg, MD 20899, USA, dale.bentz@nist.gov.

[4]Associate Professor of Civil Engineering, Lyles School of Civil Engineering, Purdue University, 550 Stadium Mall Dr., West Lafayette, IN 47907, zavattie@purdue.edu.

[5]Jack and Kay Hockema Professor of Civil Engineering and Director of the Pankow Materials Laboratory, Lyles School of Civil Engineering, Purdue University, 550 Stadium Mall Dr., West Lafayette, IN 47907, wjweiss@purdue.edu.

ABSTRACT

In North America, some concrete pavements and sidewalks have shown severe damage during freezing. The damage may increase as deicing salts (e.g. NaCl) are added to the surface of pavement in order to melt ice and snow due to the addition of osmotic/crystallization pressure or/and chemical reaction. Research has been performed to better understand the cause of damage. A test device (called longitudinal guarded comparative calorimeter (LGCC)) has been developed to assess the damage. This paper discusses the influence of rate at which the temperature of a concrete element is decreased/increased on the damage that develops in the LGCC test. Different cooling/heating rates were applied to freeze/thaw mortar specimens containing different concentrations of NaCl deicing salt. The heat flow and phase changes were monitored during the test. Damage development was determined using ultrasonic wave speed. It was observed that the rate of cooling/heating can alter the freeze-thaw damage as does the concentration of the solution in the pores (NaCl). For samples saturated with solution with concentrations less than 5 % NaCl (by mass), it seems that the rate of temperature change has a relatively insignificant effect on damage development. For samples saturated with solutions containing NaCl equal to or greater than 5 % by mass, however, an increase in damage was observed for samples tested with a faster rate. A finite difference model was also used to describe how different cooling/heating rates may influence the thermal response of the test. The results obtained from numerical simulation were in good agreement with experimental results.

Keywords: cementitious material, deicing salt, freeze-thaw, heating/cooling rate, mortar, thermal behavior

INTRODUCTION

Concrete elements may experience premature deterioration during freezing and thawing. The rate and range of temperature change, the chemical reaction between deicing salts and cementitious binders, the saturation state of the concrete, and the salt crystallization in the concrete pores may influence freeze-thaw performance. The degree of saturation of the concrete can have a considerable influence on the damage development in concrete (Fagerlund 1973; Li et al. 2012; Farnam et al. 2014d). For concrete with a degree of saturation less than the critical degree of saturation (~ 86 %), the concrete will exhibit little if any damage development, while a concrete with a degree of saturation greater than the critical degree of saturation will develop damage (Fagerlund 1973; Li et al. 2012; Farnam et al. 2014d). The addition of deicing salt can also increase the degree of saturation in concrete pores (Spragg et al 2011) or a change of the pore solution concentration that depresses the freezing temperature (Farnam et al. 2014b). The deicing salts can increase the freeze-thaw damage due to the combination of hydraulic pressure, osmotic pressure, crystallization pressure, and the pressure due to chemical reactions with the cementitious matrix (Farnam et al. 2014c; Farnam et al. 2014e; Villani et al. 2014; Qian et al. 2014). In addition, deicing salt can change the thermal properties of the concrete such as density, thermal conductivity, and specific heat capacity (Esmaeeli et al. 2014), thereby altering heat flow state in concrete under thermal cycling.

There are different techniques to measure the thermal behavior of cement paste or mortar such as low temperature differential scanning calorimetry (Litvan 1976; Beddoe and Setzer 1988; Beddoe and Setzer 1990; Farnam et al. 2014a). Despite the ability of this technique to accurately measure heat flows that can be used to identify different phase transitions, the small size of samples prohibits the testing of composite systems containing fine and coarse aggregates. A longitudinal guarded comparative calorimeter (LGCC) can be used to quantify the heat flow and thermal properties of mortar or concrete samples with larger geometry (ASTM 2009; Farnam et al. 2014a; Farnam et al. 2014b).

In this research, LGCC is used to quantify the heat flow in mortar samples. A theoretical model is developed based on the heat transfer formulations (Incropera et al. 2007) to predict and simulate phase transformations and heat transfer in materials (Lecomte and Mayer 1985; Costa et al. 1998; Velraj et al. 1999; Bentz 2000; Bentz and Turpin 2007). Experiments with different rates of temperature change were performed using LGCC to study freeze-thaw behavior of mortar. The finite difference method was used to simulate the experiment. While the degree of saturation was kept at 100 %, the effects of different concentrations of NaCl solutions and different rates of temperature change on the thermal response of mortar samples were investigated numerically and experimentally.

EXPERIMENTAL PROGRAM

Sample preparation. All experiments were performed using a mortar mixture with a water-to-cement ratio (*w/c*) of 0.42 by mass and a sand volume fraction of 55 %. The mortar contained ordinary Type I portland cement (OPC) with a Blaine fineness of 375 m^2/kg. The aggregate was natural sand with a maximum size of 4.75 mm, specific gravity of 2.61, fineness modulus of 2.89, and an absorption value of 2.2 % by mass. The mortar samples were cast as rectangular prisms (25.4 mm × 25.4 mm × 279.4 mm with ± 1 mm precision) and were sealed cured for 42 d. Following curing, samples measuring 25.4 mm × 25.4 mm × 50.8 mm (with ± 1 mm precision) were cut and then placed in a vacuum oven at 60 °C ± 1 °C for 7 d to remove their moisture. After drying, samples were fully saturated a using vacuum saturation technique with deionized (DI) water or NaCl solution (3 %, 5 %, 8 % or 10 % salt concentration by mass). After conditioning and before the freeze-thaw experiment, all sides of the sample were wiped dry and wrapped in a thin plastic sheet to minimize moisture exchange.

Freeze-thaw testing. A low-temperature longitudinal guarded comparative calorimeter (LGCC) was used to investigate thermal response of mortar sample which is shown in Figure 1a (Farnam et al. 2014a; Farnam et al. 2014c; Farnam et al. 2014b). The LGCC is used to produce a one-dimensional heat flow throughout the sample by using: (1) a longitudinal guard having approximately the same temperature gradient, and (2) thermal insulations, and an approximate heat flow can be measured. The heat flow data can be used as an indication of phase changes. In addition to identifying the phase change that occurs, damage can be monitored using the reduction in dynamic elastic modulus as detected from the change in the compressional wave speed with two coupled acoustic emission (AE) sensors. AE activity due to cracking generated throughout an LGCC experiment can be also monitored by using one AE sensor attached to the samples inside the experimental setup. In this study, one single cooling and heating cycle (shown in Figure 1b) was used which varied between 24 °C and -40 °C with different rates of temperature change during heating and cooling as shown in Table 1. A cold plate at the bottom of the LGCC experiment was used to apply different cooling/heating rates. According to the data obtained for the samples tested in this study and elsewhere (Farnam et al. 2014a; Farnam et al. 2014c; Farnam et al. 2014b), the LGCC experiment has an average coefficient of variation equal to 15.4 % for reduction in dynamic elastic modulus measurement, and 8.6 % for total released heat during freezing or thawing.

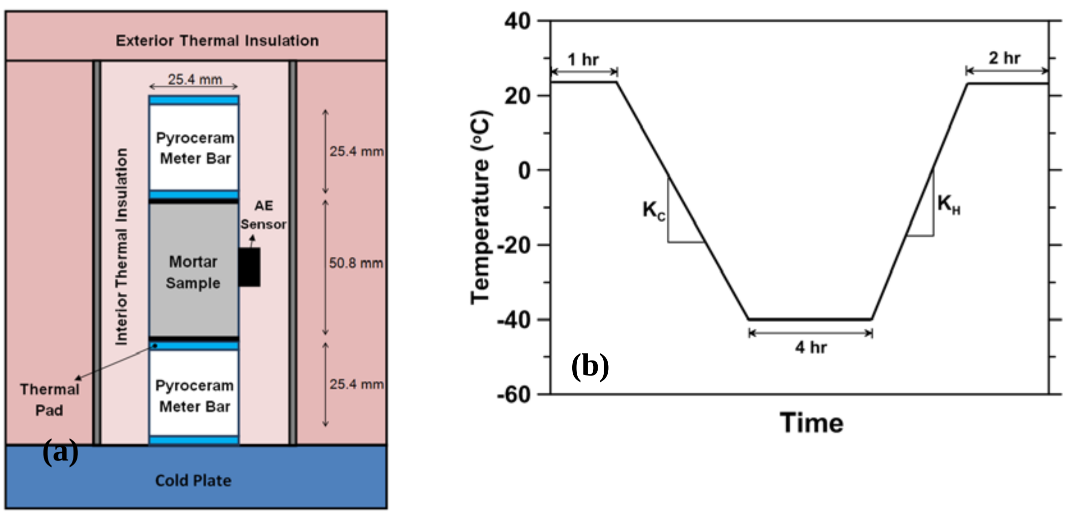

Figure 1. a) LGCC experimental setup, and b) schematic of temperature change in the cold plate in LGCC Test. Values of K_C and K_H are provided in Table 1.

Table 1. Cooling/heating rate for LGCC experiment.

Item	Temperature Change Rate (°C/h)*		
	Slow	Medium	Fast
Cooling Rate (K_C)	1	2	4
Heating Rate (K_H)	2	4	8

* The cooling and heating rates were chosen according to the time allowed during LGCC experiment and other temperatures and conditions can be applied for freezing and thawing tests.

NUMERICAL SIMULATION

A finite difference model for the system's energy balance (shown in Equation 1) was developed to calculate the temperature evolution in the sample (Bentz 2000). The model was implemented in the C programming language.

$$k_m \cdot \frac{\partial^2 T}{\partial x^2} + \frac{\partial q}{\partial t} = \rho_m \cdot C_m \cdot \frac{\partial T}{\partial t} \quad (1)$$

where k_m is the thermal conductivity of mortar sample, $T(x)$ is the temperature at distance x within the mortar sample and time t in the numerical simulation, q is the latent heat released/absorbed during a phase transformation, ρ_m is the density of mortar sample, and C_m is the specific heat capacity of the mortar sample.

The thermal properties of the modeled mortar specimen (i.e., k_m, q, ρ_m, and C_m) during cooling and heating were obtained using thermal properties of the individual constituents (dry mortar and pore solution) (Esmaeeli et al. 2014). The thermal properties used in this study are shown in Table 2 for samples saturated with DI water and 5 % NaCl solution. To predict k_m, ρ_m, and C_m during cooling and heating of mortar samples, the total freezable volume fraction of absorbed solution in mortar was considered to be 36 % by volume of the mortar sample, obtained using a desorption isotherm (Esmaeeli et al. 2014). An effective medium theory (Levy and Stroud 1997) was used to obtain k_m, while the rule of mixtures (Askeland et al. 2010) was used to obtain ρ_m and C_m. The gradual ice formation for NaCl solution was considered using the lever rule from the NaCl-H_2O phase diagram (Esmaeeli et al. 2014).

When the solution froze in the mortar sample, undercooling (i.e., freezing of a liquid at a temperature lower than its characteristic melting temperature (Debenedetti and Stanley 2003)) was observed. The undercooling was simulated in the model by considering a sudden freezing. For solution melting in the mortar sample, however, a gradual melting at a constant temperature was considered, consistent with experimental observations. The initial temperature of the entire LGCC experiment (at time equal to zero) was set to be + 24 °C. The temperature of the interface between the bottom Pyroceram and the cold plate was varied according to different rates employed in experimental program (Table 1), and the heat transfer equation (Equation 1) was solved for each time step. Temporal and spatial sizes were considered to be 0.05 s and 1 mm, respectively. These discretized sizes provided numerical convergence using the Von Neumann criterion (Isaacson 1994).

Table 2. Material properties used for numerical simulation for samples saturated with DI water and 5 % NaCl solution.

Mortar thermal properties	DI water		5 % NaCl solution	
	Before freezing	After freezing	Before freezing	After freezing
Thermal conductivity[W/(m·K)]	1.43	1.80	1.42	1.42 to 1.80*
Density [kg/m^3]	2288	2274	2295	2295 to 2274*
Specific heat capacity[J/(kg·K)]	914	717	901	901 to 717*
Melting temperature, T_m [°C]	0		-3	
Freezing temperature, T_F [°C]**	-5.5		-10.8	

* Lever rule was used to obtain the thermal properties of mortar samples saturated with NaCl solution after freezing.

** Due to undercooling effect, the freezing temperature was lower than the melting temperature for both solutions.

RESULTS AND DISCUSSION

Thermal response of mortar samples during LGCC experiment. Heat flow responses for the mortar samples were obtained using the LGCC and are shown as a function of temperature for samples saturated with DI water and 5 % NaCl solution in Figure 2. The temperature at which freezing (ice formation) occurred is lower than the temperature at which thawing (ice melting) occurred due to the undercooling effects. Changes in the heating/cooling rate seem to have only a small effect on changing the freezing and thawing temperatures within the testing regime applied in this study.

Freezing and thawing peaks become broader for samples tested with a fast rate, while they become sharper and narrower for a slower rate. In addition, heating and cooling baselines move toward each other as the rate of temperature change decreases. This is mainly due to the fact that at a slower rate, heat flow has sufficient time to diffuse throughout the sample. At a slower rate, the thermal response of a sample may best approach the steady state thermal condition and the LGCC accuracy for phase change detection increases (ASTM 2009; Farnam et al. 2014a; Farnam et al. 2014b). As the cooling/heating rate increases, the time at which temperature change occurs decreases and the heat absorption/release due to freezing/melting cannot redistribute within the sample, thereby increasing the temperature gradient throughout the sample.

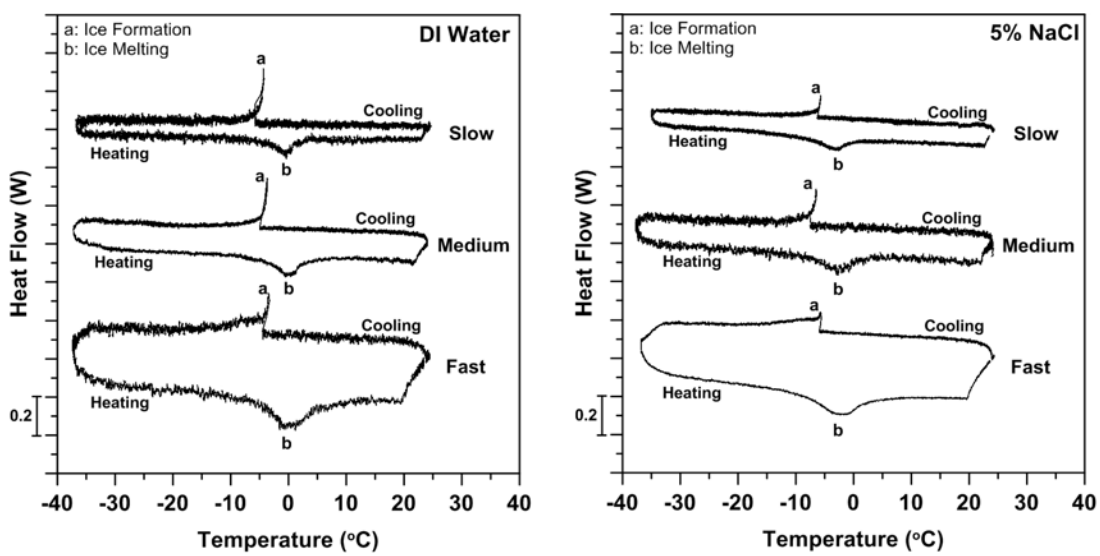

Figure 2. Effect of cooling/heating rate on thermal behavior of mortar samples saturated with deionized water (left) and solution containing 5 % NaCl (right).

Reduction in dynamic elastic modulus for mortar samples during LGCC experiment. The reduction in dynamic elastic modulus (D) for mortar samples due to freeze-thaw damage was calculated with the wave velocity using Equation 2.

$$D = 1 - \left(\frac{V_t}{V_o}\right)^2 \qquad (2)$$

where V_t and V_o are average wave velocity through the length of the sample after and before a freeze-thaw cycle in the LGCC, respectively. Figure 3 indicates the reduction in dynamic elastic modulus as a function of salt concentration for samples tested at different rates of cooling/heating (i.e., slow, medium, and fast).

Independent of the change in cooling/heating rate, it seems that the damage increases as the salt concentration increases up to 5 % and then decreases beyond this point. A higher level of damage at 5 % NaCl concentration by mass may be similar to what was observed during scaling tests, where more damage occurred because of a pessimum salt concentration between 3 % and 5 % NaCl (Valenza and Scherer 2005).

Changes in cooling/heating rate appear to have a relatively negligible influence on freeze-thaw damage for samples saturated with concentrations less than 5 % NaCl. However, a slight increase in damage can be seen for samples tested at a fast rate for concentrations equal to or greater than 5 % NaCl. For samples saturated with NaCl solution, osmotic pressure resulting from partial freezing of solutions in the pores (Powers 1958) is another source of deterioration in mortars under freezing and thawing, in addition to hydraulic pressure due to expansion resulting from ice formation. As discussed earlier, at a higher rate, heat flow does not have sufficient time to diffuse throughout the sample and the heat absorption/release due to freezing/melting cannot redistribute within the sample in the provided time. As a result, the temperature gradient throughout the sample increases. The increase in temperature gradient throughout the sample may increase the osmotic pressure and cause more damage in the samples tested with a higher cooling/heating rate.

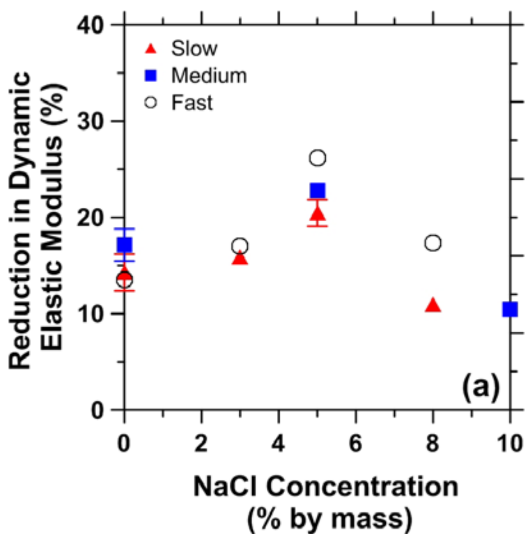

Figure 3. Reduction in dynamic elastic modulus as a function of salt concentration for samples tested at different rates of cooling/heating (Error bars indicate ± one standard deviation for two replicates).

Thermal response of mortar samples using finite difference method. The heat transfer formulation (equation 1) was employed to predict the amount of heat flow throughout the mortar samples. The thermal response of mortar samples predicted by the numerical model is shown for samples saturated with DI water and 5 % NaCl solution in Figure 4 as a function of average temperature of the sample. As seen in the experimental program, heating and cooling baselines again move toward each other as the rate of temperature change decreases, since there is enough time for heat to diffuse throughout the sample. Mortar samples exposed to DI water solution have a larger peak in comparison to the samples exposed to 5 % NaCl solution since a portion of solution is replaced by NaCl salt.

The predicted exothermic peak (associated with freezing) is relatively sharper in samples with a slow cooling/heating rate (Figure 4). This may be due to the freezing of the entire freezable solution in the mortar sample, since there is a low gradient of temperature between the top and bottom surfaces of the sample. Figure 5 indicates the temperature profile in the model mortar sample at three moments: before freezing (time t_1), during freezing (time t_2), and after freezing (time t_3). The freezing occurs right after time t_1 when the temperature of the bottom surface of the mortar sample reaches T_F (i.e., -5.5 °C from Table 2). At time t_2, most of the freezable water in the mortar sample exposed to a slow rate is frozen; as a result the temperature of the mortar at its top surface begins to fall below T_m (i.e., 0 °C from Table 2). The mortar sample exposed to a fast rate however still experiences the freezing at time t_2 since the temperature within half of the mortar sample remains at T_m. At time t_3, the freezing is completed and redistribution of heat is occurring. The freezing occurs in a relatively shorter period of time for samples exposed to a slow rate in comparison to a sample tested with a fast rate. As a result, the entire latent heat of the mortar sample will be released relatively quickly for the slow rate.

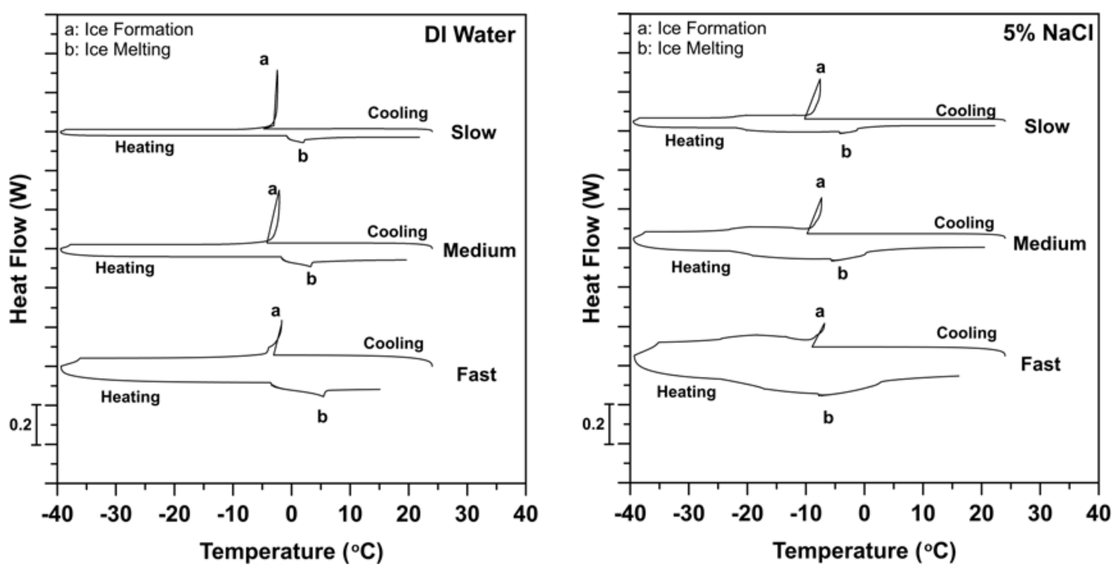

Figure 4. Heat flow as a function of temperature predicted with numerical simulation for samples saturated with deionized water (left) and a solution containing 5 % NaCl (right) under different rates of thermal cycling.

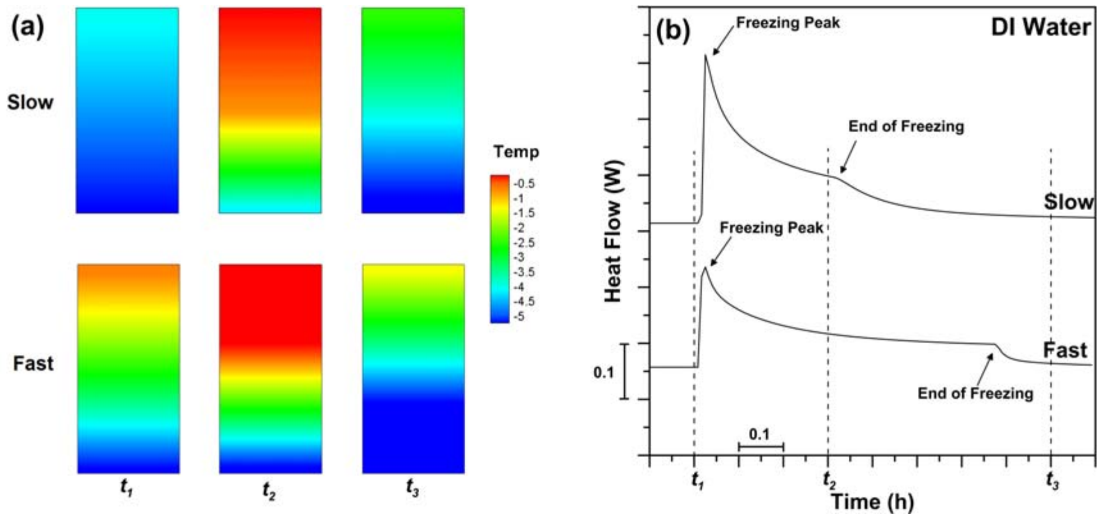

Figure 5. a) Temperature contour within mortar sample saturated with deionized water before freezing (time t_1), during freezing (time t_2), and after freezing (time t_3), and b) heat flow as a function of time for the model mortar samples saturated with DI water in the moment of freezing.

Experimental and numerical comparison. As shown in Figure 3, an increase in damage was observed for the sample saturated with solutions containing NaCl concentrations greater than 5 % tested with a higher cooling/heating rate which may be due to an additional damage caused by osmotic pressure. The osmotic pressure is mainly due to a partial freezing in mortar samples and may increase as the salt concentration increases. The numerical simulation predicts a greater difference in temperature change during freezing (shown in Figure 5a for time t_2) throughout the sample tested at a fast rate than one tested at a slower rate. The increase in temperature gradient for the sample tested in a fast rate produces a greater partial freezing in the mortar samples, increasing the damage caused by osmotic pressure. The increase in damage may not be seen for samples saturated with lower concentrations (< 5 % by mass), since the salt concentration may not be enough to create a considerable amount of osmotic pressure. For a sample saturated with higher concentrations (> 5 % by mass), however, the salt concentration reaches a level such that an increase in the temperature gradient can cause a considerable amount of osmotic pressure that can further result in an increase in damage.

As the pore solution within a saturated mortar sample begins to freeze, the latent heat of fusion is released due to ice formation. Mortar samples saturated with DI water release the latent heat corresponding to the specific heat of fusion for water, i.e., 334 J/g, while a lesser amount of heat is released during ice formation for samples saturated with NaCl solution. In fact, the heat release for samples saturated with NaCl solution is a combination of ice formation (latent heat of fusion equal to 334 J/g) and formation of a eutectic composition (latent heat of fusion equal to 245 J/g) (Esmaeeli et al. 2015). As a result, the amount of released heat due to solidification decreases as the salt concentration increases in the solution since water is replaced by NaCl salt.

Figure 6 shows the average amount of released heat during cooling due to solidification of pore solutions containing different sodium chloride concentrations obtained from the numerical simulation and from the LGCC experiment. The numerical simulation predicts a relatively higher amount of heat release during freezing in comparison to the LGCC experiment. The difference between numerical results and obtained experimental data (which is approximately 25 %) may be most likely due to: 1) heat dissipation during experimental measurement, and 2) the assumption of a steady state heat flow condition to calculate heat flow in the LGCC experiment which is not true until a very slow cooling/heating rate is used to reach steady state heat flow conditions (Esmaeeli et al. 2015). As the cooling/heating rate decreases, the amount of released heat slightly increases in the experiment and moves toward the results predicted by numerical simulation since relatively a steady-state may be reached. As shown in Figure 6b for the sample saturated with 5 % NaCl solution, the released heat comes closer to the predicted value as the cooling/heating rate decreases. In general, a good agreement is seen between numerical simulation and experimental results comparing the average amount of released heat during cooling.

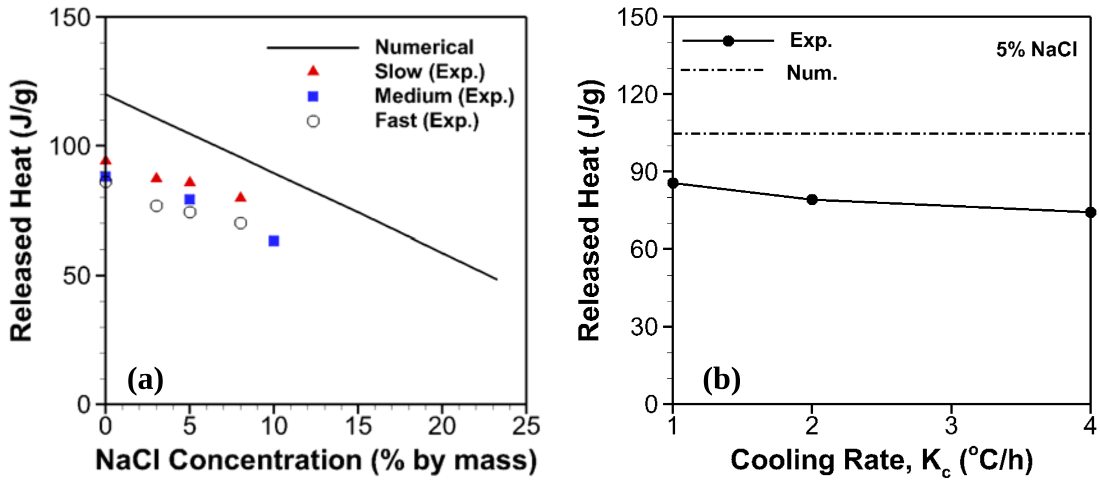

Figure 6. a) Amount of released heat during cooling due to solidification of pore solutions containing different sodium chloride concentrations, and b) amount of released heat for samples saturated with 5% NaCl solution as a function of cooling rate (the released heat measurement had an average coefficient of variation equal to 8.6 %).

SUMMARY AND CONCLUSION

Experimental and numerical approaches were used in this paper to describe how the rate of temperature change can influence the freeze-thaw behavior in mortar samples saturated with NaCl solution. For samples saturated with solution with concentrations less than 5 % NaCl (by mass), it seems that the freeze-thaw cycling rate has a relatively insignificant effect on damage development. For samples saturated with solutions containing NaCl equal to or greater than 5 % by mass, however, an increase in damage was observed for samples tested with a fast rate. This is due to the fact that samples tested at a fast rate experienced a higher temperature gradient throughout the sample in comparison to samples tested at a slower rate as predicted using a numerical simulation. As a result, the higher temperature gradient may cause an increase in osmotic pressure for samples saturated with solutions containing NaCl equal to or greater than 5 % by mass, resulting in more damage. Changes in the cooling/heating rate can also alter the heat flow response, since at a slower rate, heat flow has enough time to diffuse throughout the sample. The results obtained from the one-dimensional finite difference numerical model provide a promising prediction for the thermal response of mortar tested under various cooling/heating rates in comparison to experimental data. The model shows that samples tested with a low cooling/heating rate may experience a thermal condition near steady state and the results obtained from such an LGCC test would be more reliable. The model can be further used to predict the thermal behavior of concrete exposed to deicing salt and different rates of temperature change.

ACKNOWLEDGEMENT

This work was supported in part by the Joint Transportation Research Program administered by the Indiana Department of Transportation and Purdue University under SPR 3523. The work described in this paper was conducted in the Pankow Materials Laboratory at Purdue University and the Accelerated Pavement Testing facility at INDOT, and the authors would like to acknowledge the support that has made its operation possible. The contents of this paper reflect the views of the authors, who are responsible for the facts and the accuracy of the data presented herein, and do not necessarily reflect the official views or policies of the Federal Highway Administration and the Indiana Department of Transportation, nor do the contents constitute a standard, specification, or regulation.

REFERENCES

Askeland, D. R., Fulay, P. P., & Wright, W. J. (2010). *The Science and Engineering of Materials*. (6th, Ed.)*ZAMM - Zeitschrift für Angewandte Mathematik und Mechanik* (Vol. 9, pp. 49–58). Cengage Learning.

ASTM. (2009). ASTM E1225- Standard test method for thermal conductivity of solids by means of the guarded-comparative-longitudinal heat flow technique. West Conshohocken, PA: ASTM International.

Beddoe, R., & Setzer, M. (1988). A low-temperature DSC investigation of hardened cement paste subjected to chloride action. *Cement and Concrete Research*, *18*(2), 249–256. http://doi.org/http://dx.doi.org/10.1016/0008-8846(88)90009-9

Beddoe, R., & Setzer, M. (1990). Phase transformations of water in hardened cement paste, a low-temperature DSC investigation. *Cement and Concrete Research*, *20*(2), 236–242. http://doi.org/http://dx.doi.org/10.1016/0008-8846(90)90076-A

Bentz, D. (2000). *A computer model to predict the surface temperature and time-of-wetness of concrete pavements and bridge decks*. US Department of Commerce, Technology Administration, National Institute of Standards and Technology.

Bentz, D. P., & Turpin, R. (2007). Potential applications of phase change materials in concrete technology. *Cement and Concrete Composites*, *29*(7), 527–532. http://doi.org/10.1016/j.cemconcomp.2007.04.007

Costa, M., Buddhi, D., & Oliva, A. (1998). Numerical simulation of a latent heat thermal energy storage system with enhanced heat conduction. *Energy Conversion and Management*, *39*(3-4), 319–330. http://doi.org/10.1016/S0196-8904(96)00193-8

Debenedetti, P. G., & Stanley, H. E. (2003). Supercooled and glassy water. *Physics Today*, *56*(6), 40–46. http://doi.org/http://dx.doi.org/10.1063/1.1595053

Esmaeeli, H. S., Farnam, Y., Bentz, D., Zavattieri, P. D., & Weiss, J. (2014). Numerical Simulations of the Freeze-Thaw Behavior of Mortar Containing Deicing Salt Solution. *Under NIST WERB Review*.

Fagerlund, G. (1973). The Signifcance of Critical Degrees of Saturation at Freezing of Porous and Brittle Materials. In *Durability of Concrete ACI SP-47* (pp. 13–66). OTTAWA. http://doi.org/10.14359/17604

Farnam, Y., Bentz, D., Hampton, A., & Weiss, J. (2014a). Acoustic Emission and Low Temperature Calorimetry Study of Freeze and Thaw Behavior in Cementitious Materials Exposed to Sodium Chloride Salt. *Transportation Research Record*, *2441*, 81–90.

Farnam, Y., Bentz, D., Sakulich, A., Flynn, D., & Weiss, J. (2014b). Measuring Freeze and Thaw Damage in Mortars Containing Deicing Salt Using a Low-Temperature Longitudinal Guarded Comparative Calorimeter and Acoustic Emission. *Advances in Civil Engineering Materials*, *3*(1), 316–337. http://doi.org/10.1520/ACEM20130095

Farnam, Y., Dick, S., Wiese, A., Davis, J., Bentz, D., & Weiss, J. (2014c). The Influence of Calcium Chloride Deicing Salt on Phase Changes and Damage Development in Cementitious Materials. *Submitted to Cement and Concrete Composite*, 1–41.

Farnam, Y., Todak, H., Spragg, R., & Weiss, J. (2015d). Electrical Response of Mortar with Different Degrees of Saturation and Deicing Salt Solutions during Freezing and Thawing. *Cement and Concrete Composites*. http://doi.org/10.1016/j.cemconcomp.2015.03.003

Farnam, Y., Wiese, A., Bentz, D., Davis, J., & Weiss, J. (2014e). Damage Development in Cementitious Materials Exposed to Magnesium Chloride Deicing Salt. *Submitted to Construction and Building Materials*.

Incropera, F. P., DeWitt, D. P., Bergman, T. L., & Lavine, A. S. (2007). *Fundamentals of Heat and Mass Transfer*. (F. P. Incropera, F. P. F. O. H. Incropera, & M. Transfer, Eds.)*Water* (Vol. 6th, p. 997). John Wiley & Sons. http://doi.org/10.1016/j.applthermaleng.2011.03.022

Isaacson, E. (1994). *Analysis of numerical methods*. Courier Dover Publications.

Lecomte, D., & Mayer, D. (1985). Design method for sizing a latent heat store/heat exchanger in a thermal system. *Applied Energy*, *21*(1), 55–78. http://doi.org/10.1016/0306-2619(85)90074-1

Levy, O., & Stroud, D. (1997). Maxwell Garnett theory for mixtures of anisotropic inclusions: Application to conducting polymers. *Physical Review B*, *56*(13), 8035–8046. http://doi.org/10.1103/PhysRevB.56.8035

Li, W., Pour-Ghaz, M., Castro, J., & Weiss, J. (2012). Water absorption and critical degree of saturation relating to freeze-thaw damage in concrete pavement joints. *Journal of Materials in Civil Engineering*, *24*(3), 299–307. http://doi.org/10.1061/(ASCE)MT.1943-5533.0000383

Litvan, G. (1976). Frost action in cement in the presence of de-icers. *Cement and Concrete Research*, *6*(September 1974), 351–356. Retrieved from http://www.sciencedirect.com/science/article/pii/0008884676900971

Powers, T. C. (1958). The physical structure and engineering properties of concrete. *Research Department Bulletin, Portland Cement Association*, *90*, 27 pages.

Qian, Y., Farnam, Y., & Weiss, J. (2014). Using Acoustic Emission to Quantify Freeze–Thaw Damage of Mortar Saturated with NaCl Solutions. In *Proceedings of the 4th International Conference on the Durability of Concrete Structures* (pp. 32–37). Purdue University Libraries Scholarly Publishing Services. http://doi.org/10.5703/1288284315379

Spragg, R. P., Castro, J., Li, W., Pour-Ghaz, M., Huang, P.-T., & Weiss, J. (2011). Wetting and drying of concrete using aqueous solutions containing deicing salts. *Cement and Concrete Composites*, *33*(5), 535–542. http://doi.org/10.1016/j.cemconcomp.2011.02.009

Valenza, J. J., & Scherer, G. W. (2005). Mechanisms of salt scaling. *Materials and Structures*, *38*(4), 479–488. http://doi.org/10.1007/BF02482144

Velraj, R., Seeniraj, R. V., Hafner, B., Faber, C., & Schwarzer, K. (1999). HEAT TRANSFER ENHANCEMENT IN A LATENT HEAT STORAGE SYSTEM. *Solar Energy*, *65*(3), 171–180. http://doi.org/10.1016/S0038-092X(98)00128-5

Villani, C., Spragg, R., Pour-Ghaz, M., & Jason Weiss, W. (2014). The Influence of Pore Solutions Properties on Drying in Cementitious Materials. *Journal of the American Ceramic Society*, *97*(2), 386–393. http://doi.org/10.1111/jace.12604